



Demonstration of a Direct Interaction between β_2 -Adrenergic Receptor and Insulin Receptor by BRET and Bioinformatics

Maja Mandić¹, Luka Drinovec², Sanja Glisic³, Nevena Veljkovic³, Jane Nøhr⁴, Milka Vrecl^{1*}

1 Institute of Anatomy, Histology & Embryology, Veterinary Faculty, University of Ljubljana, Ljubljana, Slovenia, **2** Development Department, Aerosol d.o.o., Ljubljana, Slovenia, **3** Center for Multidisciplinary Research, Institute of Nuclear Sciences VINCA, University of Belgrade, Belgrade, Serbia, **4** Department of Incretin & Islet Biology, Novo Nordisk A/S, Måløv, Denmark

Abstract

Glucose metabolism is under the cooperative regulation of both insulin receptor (IR) and β_2 -adrenergic receptor (β_2 AR), which represent the receptor tyrosine kinases (RTKs) and seven transmembrane receptors (7TMRs), respectively. Studies demonstrating cross-talk between these two receptors and their endogenous coexpression have suggested their possible interactions. To evaluate the effect of IR and prospective heteromerization on β_2 AR properties, we showed that IR coexpression had no effect on the ligand binding properties of β_2 AR; however, IR reduced β_2 AR surface expression and accelerated its internalization. Additionally, both receptors displayed a similar distribution pattern with a high degree of colocalization. To test the possible direct interaction between β_2 AR and IR, we employed quantitative BRET² saturation and competition assays. Saturation assay data suggested constitutive β_2 AR and IR homo- and heteromerization. Calculated acceptor/donor (AD₅₀) values as a measure of the relative affinity for homo- and heteromer formation differed among the heteromers that could not be explained by a simple dimer model. In heterologous competition assays, a transient increase in the BRET² signal with a subsequent hyperbolic decrease was observed, suggesting higher-order heteromer formation. To complement the BRET² data, we employed the informational spectrum method (ISM), a virtual spectroscopy method to investigate protein-protein interactions. Computational peptide scanning of β_2 AR and IR identified intracellular domains encompassing residues at the end of the 7th TM domain and C-terminal tail of β_2 AR and a cytoplasmic part of the IR β chain as prospective interaction domains. ISM further suggested a high probability of heteromer formation and homodimers as basic units engaged in heteromerization. In summary, our data suggest direct interaction and higher-order β_2 AR:IR oligomer formation, likely comprising heteromers of homodimers.

Citation: Mandić M, Drinovec L, Glisic S, Veljkovic N, Nøhr J, et al. (2014) Demonstration of a Direct Interaction between β_2 -Adrenergic Receptor and Insulin Receptor by BRET and Bioinformatics. PLoS ONE 9(11): e112664. doi:10.1371/journal.pone.0112664

Editor: Laszlo Buday, Hungarian Academy of Sciences, Hungary

Received: June 7, 2014; **Accepted:** October 6, 2014; **Published:** November 17, 2014

Copyright: © 2014 Mandić et al. This is an open-access article distributed under the terms of the Creative Commons Attribution License, which permits unrestricted use, distribution, and reproduction in any medium, provided the original author and source are credited.

Data Availability: The authors confirm that all data underlying the findings are fully available without restriction. All relevant data are within the paper and its Supporting Information files.

Funding: The authors acknowledge funding from the Basileus S Program to M. Mandić, the Slovenian Research Agency program (P4-0053) to M. Vrecl, and the Ministry of Education, Science and Technological Development of the Republic of Serbia (Grant No. 173001) to S. Glisic and N. Veljkovic. M. Vrecl, S. Glisic and N. Veljkovic participate in the European COST Action CM1207 (GLISTEN). The funders had no role in the study design, data collection and analysis, decision to publish, or preparation of the manuscript.

Competing Interests: It is true that two coauthors are employed by commercial companies; however this does not alter the authors' adherence to PLOS ONE policies on sharing data and materials. The competing interests and financial disclosures of both co-authors employed by commercial companies are as follows: Luka Drinovec is employed by the company Aerosol d.o.o. This company produces instruments for the measurement of aerosolized soot (black carbon) and some accessories for aerosol measurement. Aerosol d.o.o. does not have any connection with molecular biology, development of medicines, etc. Thus, the authors declare that there are no competing interests for Luka Drinovec coauthoring the article "Demonstration of a direct interaction between β_2 -adrenergic receptor and insulin receptor by BRET and bioinformatics". Response to Reviewers: Jane Nøhr is employed by Novo Nordisk A/S and owns Novo Nordisk A/S company stocks. The work on this paper was done as a part of collaboration with academia, i.e., co-supervision of Maja Mandić at the Veterinary faculty, University of Ljubljana. Therefore, the authors declare that there are no competing interests for Jane Nøhr coauthoring the article, "Demonstration of a direct interaction between β_2 -adrenergic receptor and insulin receptor by BRET and bioinformatics".

* Email: milka.vrecl@vf.uni-lj.si

Introduction

The functional interplay between different classes of receptors represents a means of fine-tuning the control of cellular functions that could be fundamental for understanding pathologic conditions and responses to therapeutic agents that interact with cell-surface receptors. Originally, 7 transmembrane receptors (7TMRs) and receptor tyrosine kinases (RTKs), together with their respective downstream effectors, were thought to represent distinct and linear signaling units; however, recent studies have

provided evidence for functional crosstalk between these different types of receptors [1].

Glucose metabolism is under the cooperative regulation of the RTK insulin receptor (IR) and β_2 -adrenergic receptor (β_2 AR), a representative 7TMR. The anabolic action of insulin promotes glycogen synthesis, glucose uptake in skeletal muscle and lipid storage. By contrast, catecholamines act in opposition to insulin, stimulating glycogen breakdown, gluconeogenesis, and lipolysis [2]. They play an important role in counter-regulation of insulin-induced hypoglycemia. The ability of insulin to counter regulate

catecholamine action at the tissue/cellular level is crucial for the “tight” regulation of serum glucose levels, and interaction between IR and β_2 AR could be a required action in this process.

At the molecular level, the ability of insulin to counter regulate β_2 ARs can be exerted through insulin-stimulated phosphorylation of β_2 AR and its subsequent internalization. An early *in vitro* study demonstrated that, in the presence of insulin, IR catalyzes the phosphorylation of β_2 AR predominantly at residues located in the cytoplasmic tail of β_2 AR—i.e., Tyr350/Tyr354, and Tyr364 [3]—a finding that was consistent with the hypothesis that IR directly interacts with and phosphorylates β_2 AR. Phosphorylated β_2 AR Tyr350 creates a phosphotyrosine Src homology 2 (SH2) binding domain, which effectively precludes β_2 AR from coupling to its cognate G-protein (G_{α_s}) and enables binding of the adaptor Grb2, the p85 regulatory subunit of phosphoinositide 3-kinase (PI3K) or the GTPase dynamin; all of the latter molecules are involved in 7TMR trafficking [4,5,6]. In addition, insulin-induced activation of MAPKs, ERK 1 and ERK 2, is potentiated by β_2 AR via a mechanism that requires the integrity of Tyr350 [4]. Thus, the functional cross-talk between β_2 AR and IR may be to fine tune the signals from multiple receptor signaling pathways. Recently, Fu et al. [7] described an IR: β_2 AR complex in the mouse heart, indicating that cross-talk between these two receptors could provide a molecular basis for the pathophysiology of metabolic and cardiovascular dysfunction under insulin-resistant states. β_2 AR and IR are also endogenously coexpressed in other cell types—i.e., pancreatic beta cells, adipocytes, liver cells, skeletal muscle cells and astrocytes [8,9,10]. Therefore, the formation of heteromeric complexes consisting of these two receptors may be plausible.

In the past decade, the concept that 7TMRs can exist as dimers or higher-order oligomers has advanced rapidly [11,12], and biophysical techniques based on resonance energy transfer (RET) such as BRET have become methods of choice in receptor oligomerization studies (recently reviewed in [13,14,15,16,17,18]). Utilizing BRET, β_2 AR homo- and heteromerization with different 7TMR family members have been reported [19,20,21,22,23,24,25].

In contrast to 7TMR-based BRET studies, BRET has been less exhaustively employed for RTK-based studies, and an overview of BRET studies associated with RTKs was recently reviewed by Issad et al. [26] and Siddiqui et al. [27]. RTKs often employ dimerization as a key factor in their activation; in fact, members of the IR subfamily are pre-dimerized by disulfide bonds (reviewed by De Meyts [28]). In IR studies, BRET was used to monitor the activation state of IR [29,30,31] and its interactions with different intracellular binding partners, including protein tyrosine phosphatase-1B [32], Grb14 [33] and IRS1, IRS4 and Shc [34]. IR can also form hybrid heterotetramers with the insulin-like growth factor-1 (IGF-1) receptor, exemplifying that IR can comprise heteromers that are products of independent genes [35].

In addition to interfamilial receptor heteromerization—i.e., 7TMR:7TMR and RTK:RTK pairs—a physiologically relevant, direct physical interaction between the 7TMR adenosine A_{2A} receptor (A_{2A} -AR) and RTK fibroblast growth factor receptor (FGFR) was demonstrated [36]. Evidence for other 7TMR:RTK complexes was also provided [37,38,39]. Computer-assisted analysis suggested that the N- and C-termini, as well as the third intracellular loop (ICL3) of 7TMRs show a propensity toward unstructured conformation, and could potentially interact with domains of other receptors/receptor-interacting proteins (reviewed in [40]).

To test whether β_2 AR and IR are prospective interaction partners, we employed the following methods: i) radioligand

binding and enzyme-linked immunosorbent assay (ELISA) to determine the receptor-binding properties and surface expression, as well as to quantify receptor internalization processes; ii) confocal microscopy to detect possible colocalization between β_2 AR and IR; iii) BRET² proximity assays consistent with the direct interaction between β_2 AR and IR; and iv) the informational spectrum method (ISM), a virtual spectroscopy method to investigate protein-protein interactions [41,42], to identify important informational characteristics of the interaction between β_2 AR and IR and to predict domains potentially involved in their interaction. Prior studies have proved this bioinformatics approach to be effective in identifying protein-protein interaction partners and some of them were also confirmed experimentally [43,44].

Materials and Methods

Materials

Molecular biology reagents, as well as the tissue culture media and reagents, were purchased from Sigma-Aldrich (St. Louis, MO, USA) and Gibco Invitrogen Corporation (Breda, the Netherlands), unless otherwise specified. [¹²⁵I]-Iodopindolol was obtained from PerkinElmer (Boston, MA, USA). The ligands pindolol and isoproterenol were purchased from Sigma-Aldrich, and recombinant human insulin S100 was from Novo Nordisk A/S (Bagsvaerd, Denmark). Coelenterazine 400a was purchased from Biotrend Chemikalien GmbH (Köln, Germany). Anti-hemagglutinin (HA) high-affinity rat monoclonal antibodies were from Roche (Basel, Switzerland). Anti-rat horseradish peroxidase (HRP)-conjugated antibodies and anti-rat TRITC-conjugated antibodies were from Sigma-Aldrich.

Receptor fusion constructs

Human HA-tagged β_2 AR (HA- β_2 AR) cDNA in the vector pcDNA3.1 was purchased from Missouri S&T cDNA Resource Center (University of Missouri-Rolla, USA). HA- β_2 AR C-terminally tagged with *Renilla luciferase* 8 (RLuc8) (β_2 AR-RLuc8) was made using standard molecular biology techniques and was verified by sequencing. WT human IR isoform A that lacks exon 11 and IR C-terminally tagged with the green fluorescent protein variant 2 (IR-GFP²) were generated and verified at Novo Nordisk A/S. C-terminally RLuc8-tagged IR (IR-RLuc8), C-terminally GFP²-tagged β_2 AR (β_2 AR-GFP²) and the membrane-inserted GFP²-tagged construct (GFP²-17aa) were the same as described previously [24,34,45]. All of the generated cDNA clones were inserted into the expression vector pcDNA3.1(+).

Cell culture and transfection

HEK-293 cells (European Collection of Animal Cell Cultures, Salisbury, UK) were routinely maintained and passaged in Dulbecco's modified Eagle's Medium (DMEM) supplemented with 10% (v/v) heat-inactivated fetal calf serum, 2 mM Glutamax-I, penicillin (100 U/mL) and streptomycin (100 μ g/mL) at 37°C in a humidified atmosphere of 5% (v/v) CO₂. For transient transfection, HEK-293 cells were seeded at a density of $\sim 1 \times 10^6$ cells per 60-mm tissue culture dish or at a density of 4×10^6 cells per 75-cm² flask and transfections were performed the following day using Lipofectamine 2000 according to the manufacturer's instructions. Cells were harvested 48 h after transfection, the cell number was determined using a cover-slipped hemocytometer, and the cells were resuspended in Dulbecco's PBS supplemented with Ca²⁺/Mg²⁺, 1 g/L glucose and 36 mg/L sodium pyruvate to a density of 1×10^6 cells/mL, unless otherwise stated.

Table 1. Pharmacological properties of β_2 AR fusion constructs expressed in HEK-293 cells.

Receptor	IC ₅₀ (nM)
HA- β_2 AR	1.58±0.26
HA- β_2 AR-RLuc8	1.16±0.11
β_2 AR-GFP ²	1.88±0.58
β_2 AR-RLuc	0.94±0.06 ^a

^aData from Vrecl et al. [47].

HEK-293 cells expressing HA- β_2 AR, β_2 AR-GFP² or HA- β_2 AR-RLuc8 were incubated with [¹²⁵I]-iodopindolol and increasing concentrations of pindolol (10⁻¹² to 10⁻⁵ M final concentration). IC₅₀ values were generated using a sigmoidal dose-response curve fit (GraphPad Prism 5.0). Data are expressed as the means ± S.E. of three independent experiments performed in triplicate.

doi:10.1371/journal.pone.0112664.t001

Luminescence and fluorescence measurements

The expression levels of RLuc8- and GFP²-tagged receptor constructs were monitored by total luminescence and fluorescence measurements as previously described [46]. For luminescence measurements, $\sim 2 \times 10^5$ of resuspended cells were distributed in 96-well microplates (white Optiplate; Packard BioScience, Meriden, CT, USA). After the addition of coelenterazine 400a to a final concentration of 5 μ M, total luminescence was measured using a TriStar LB 942 microplate reader (Berthold Technologies, Bad Wildbad, Germany). For fluorescence measurements, $\sim 2 \times 10^5$ of resuspended cells from the same transfections were plated in black 96-well FIA plates (Greiner Bio-One, Frickenhausen, Germany). Total fluorescence was measured using the TriStar LB 942 microplate reader with an excitation filter at 380 nm and an emission filter at 515 nm. Background values obtained with mock-transfected HEK-293 cells were subtracted in both measurements, and the mean values of triplicate wells/sample were then calculated.

Receptor Binding Assay

To establish a relationship between the luminescence/fluorescence signals generated by RLuc8 and GFP²-tagged β_2 ARs and cell-surface receptor number, radioligand binding assays were carried out on whole cells as previously described [47]. After transfections with increasing amounts of cDNA (0.01 to 2 μ g) for either β_2 AR-RLuc8 or β_2 AR-GFP², cells were plated onto 24-well plates at a density of $\sim 1 \times 10^5$ cells per well. An aliquot of cells ($\sim 5 \times 10^5$) from each transfection was also transferred into a 60-mm dish for total luminescence/fluorescence measurements as described above. For the whole-cell radioligand binding assay, cells were washed once with assay buffer (HEPES-modified

DMEM with 0.1% bovine serum albumin (BSA)) before being incubated with the β_2 AR antagonist [¹²⁵I]-iodopindolol (30,000 cpm/well) and increasing concentrations of unlabeled pindolol (10⁻¹² to 10⁻⁵ M final concentration) in assay buffer for 2 h at 4°C. Cells were then washed 3 times with ice-cold PBS and solubilized with 0.2 M NaOH and 1% sodium dodecyl sulfate (SDS) solution, and then the radioactivity levels were determined using a γ counter (LKB Wallac, Turku, Finland). Determination of the radioactivity levels was performed in triplicate. Binding parameters were determined from displacement curves generated by a sigmoidal dose-response curve fit (GraphPad Prism 5.0). Receptor density (B_{max}), expressed as the receptor number per cell, was calculated as previously described by Ramsay et al. [48]. Whole-cell radioligand binding assays were also performed with cells expressing β_2 AR alone or in combination with IR. Displacement curves were generated using [¹²⁵I]-iodopindolol (30,000 cpm/well) and increasing concentrations of isoproterenol or isoproterenol and insulin, and IC₅₀ values were then determined using GraphPad Prism 5.0.

ELISA

ELISA assays for the measurement of surface-expressed HA- β_2 AR and quantification of receptor internalization were performed as described previously [49]. Briefly, HEK-293 cells were transiently transfected with either β_2 AR-RLuc8 alone or β_2 AR-RLuc8 and IR-GFP². One microgram of each receptor was used, and the total amount of cDNA used for transfection was kept uniform by adding empty pcDNA3.1 vector. After transfection, cells were seeded at a density of $\sim 1 \times 10^5$ cells per well in a 24-well plate. An aliquot of cells ($\sim 5 \times 10^5$) from each transfection was also transferred into a 60-mm dish for total luminescence/fluorescence

Table 2. Effect of IR coexpression on the pharmacological properties of β_2 AR in HEK-293 cells.

Ligands	IC ₅₀ (nM)	
	HA- β_2 AR	HA- β_2 AR+IR
pindolol	1.58±0.26	1.15±0.15
isoproterenol	576.7±134.2	406.5±36.5
insulin	ND	ND
pindolol+insulin	2.73±0.58	1.13±0.23

ND – not detected.

HEK-293 cells expressing HA- β_2 AR alone or HA- β_2 AR together with IR at a 1:1 cDNA ratio were incubated with [¹²⁵I]-iodopindolol and increasing concentrations of the indicated ligands (10⁻¹² to 10⁻⁵ M final concentration). When the concomitant effect of pindolol and insulin was tested, insulin was added to a 0.1 μ M final concentration. IC₅₀ values were generated using a sigmoidal dose-response curve fit (GraphPad Prism 5.0). Data are expressed as the means ± S.E. of three independent experiments performed in triplicate.

doi:10.1371/journal.pone.0112664.t002

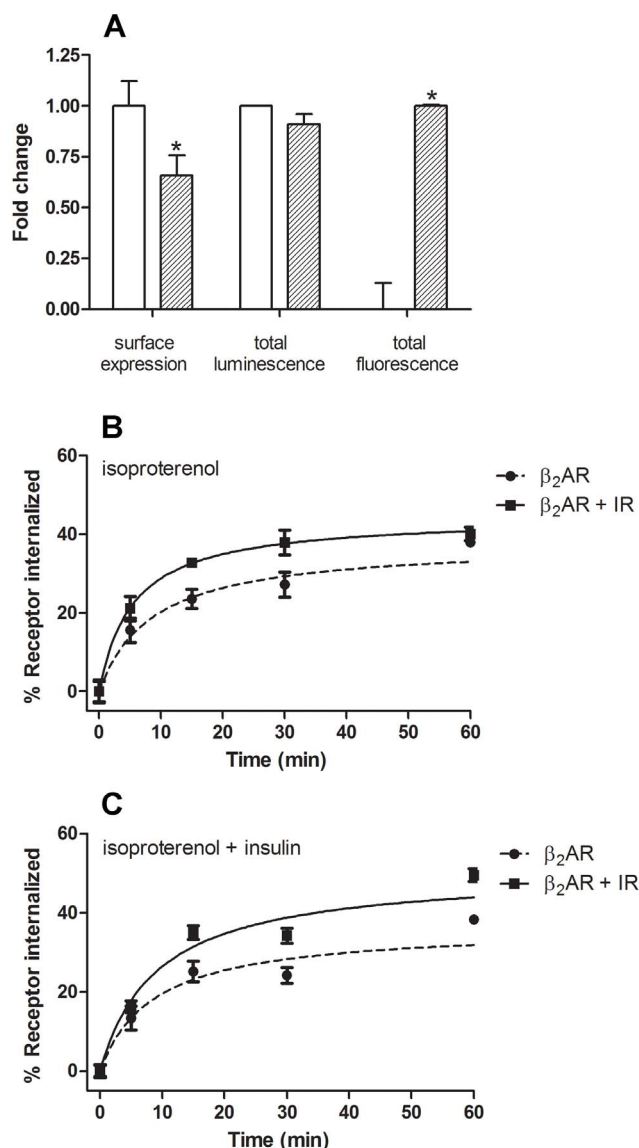


Figure 1. Effect of IR coexpression on β_2 AR surface expression and internalization in HEK-293 cells. **(A)** ELISA was performed on intact HEK-293 cells transiently transfected with HA- β_2 AR-RLuc8 alone (open bars) or HA- β_2 AR-RLuc8 together with IR-GFP² (hatched bars) at a 1:1 cDNA ratio using an antibody directed against the HA epitope. Antibody binding, as an index of receptor surface expression, was determined by measuring the absorbance at 450 nm. HA- β_2 AR-RLuc8 and IR-GFP² total relative expression was determined by luminescence and fluorescence measurement, respectively. Total luminescence was measured after the addition of the RLuc substrate coelenterazine 400a. Total fluorescence was measured with an excitation filter at 380 nm and an emission filter at 515 nm. Fold change is relative to open bars for surface expression and total luminescence, and relative to hatched bars for total fluorescence. Data are expressed as the means \pm S.E. of three independent experiments performed in triplicate. *, $p < 0.05$ as compared with HA- β_2 AR-RLuc8 transfected cells. **(B, C)** Effect of IR coexpression on the time-course of β_2 AR internalization. HEK-293 cells were transiently transfected with either β_2 AR (dotted line) or β_2 AR together with the IR (solid line) at a 1:1 cDNA ratio. β_2 AR internalization was first induced by (B) isoproterenol (10 μ M) or (C) the combination of isoproterenol (10 μ M) and insulin (0.1 μ M) for the indicated time intervals. Receptor sequestration was then defined as the decrease in specific [¹²⁵I]-iodopindolol binding compared with the total binding obtained in untreated cells. The amount of internalized receptors as a function of time was fitted using a one-site binding (hyperbola) curve fit

(GraphPad Prism 5.0). Data are expressed as the means \pm S.E. from three independent experiments performed in triplicate. doi:10.1371/journal.pone.0112664.g001

measurements as described above. After 48 h, cells were first subjected to a 2-h starvation period, and then were treated as required in HEPES-modified DMEM with 0.1% BSA for 30 min at 37°C before fixing with 4% paraformaldehyde for 20 min at 4°C. Cells were then washed 3 times in PBS and blocked (PBS containing 1% BSA) for 60 min at room temperature. Cells were kept at room temperature for all of the subsequent steps. First, cells were incubated for 2 h with anti-HA antibody at a 1:600 dilution. After 3 washes, cells were incubated with anti-rat horseradish peroxidase-conjugated antibody at a 1:1000 dilution. After extensive washing, the reaction was developed using the 3, 3', 5, 5'-tetra-methylbenzidine (TMB) liquid substrate system. The enzymatic reaction was stopped after 30 min at 37°C by adding 0.2 N sulfuric acid. The absorbances were measured at 450 nm using the microplate reader Rosys Anthos 2010 (Anthos Labtec Instruments, Wals, Austria). Determinations were made in triplicate.

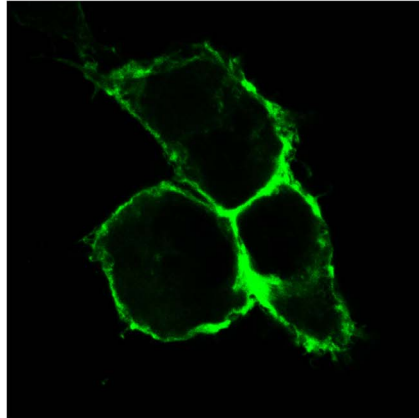
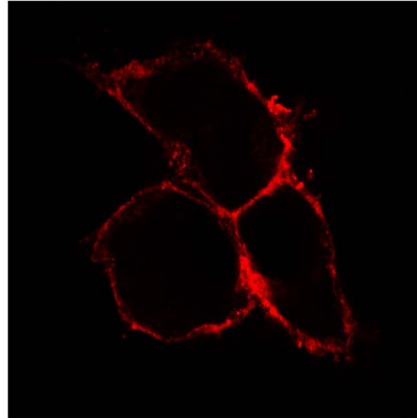
Receptor internalization assay

The β_2 AR internalization assay was performed as described previously [47]. Briefly, HEK-293 cells were transiently transfected with either β_2 AR alone or β_2 AR and IR. One microgram of each receptor was used, and the total amount of cDNA used for transfection was kept uniform by adding empty pcDNA3.1 vector. After 2 days, cells were first subjected to a 2-h starvation period in assay medium (HEPES-modified DMEM with 0.01% BSA) before being incubated with 10 μ M isoproterenol or a combination of 10 μ M isoproterenol and 0.1 μ M insulin S100 in assay medium for time intervals ranging from 5 min to 60 min at 37°C. Cells were then placed on ice, washed 3 times with ice-cold PBS and incubated for 2 h with [¹²⁵I]-iodopindolol in the presence or absence of 10 μ M pindolol at 4°C. Specific binding in each fraction was determined as the difference between radiolabeled ligand detected in the presence and absence of 10 μ M pindolol. Receptor sequestration was then defined as the decrease in specific [¹²⁵I]-iodopindolol binding compared with the total binding obtained in untreated cells. The amount of internalized receptors as a function of time was fitted using a one-site binding (hyperbola) curve fit (GraphPad Prism 5.0) to estimate the half-time of internalization ($t_{1/2}$). All of the time points were performed in triplicate.

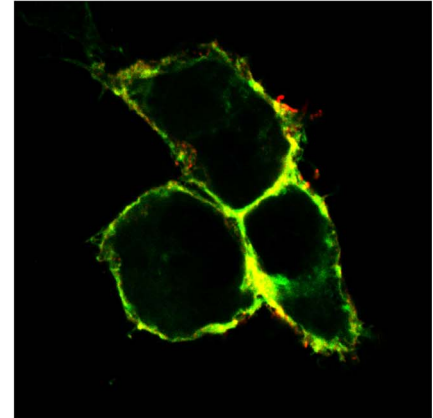
Confocal microscopy

HEK-293 cells were transiently transfected with constructs encoding HA-tagged and/or GFP²-tagged receptor constructs, trypsinized, and plated on poly-L-lysine-coated glass coverslips in complete DMEM. After 48 h, cells were treated as required with either 10 μ M isoproterenol, 0.1 μ M insulin S100 or the combination of both in HEPES-modified DMEM for 10 min at 37°C. Upon treatment, cells were washed with ice-cold PBS and fixed with 4% paraformaldehyde for 20 min at 4°C. Following washing (3 times in PBS), cells were permeabilized with PBS containing 0.01% Triton X-100 for 20 min. To reduce the nonspecific binding, cells transfected with the HA-tagged receptors were incubated in blocking solution (PBS containing 1% BSA) for 30 min. Subsequently, cells were incubated with a 1:100 dilution of primary rat anti-HA antibodies in PBS overnight at 4°C. Following washing (3 times in PBS), cells were incubated with a 1:50 dilution of secondary rabbit anti-rat TRITC-conjugated antibodies for 60 min at room temperature in the dark. Cells were

Untreated cells

IR-GFP² β_2 AR

overlay



Isoproterenol + insulin

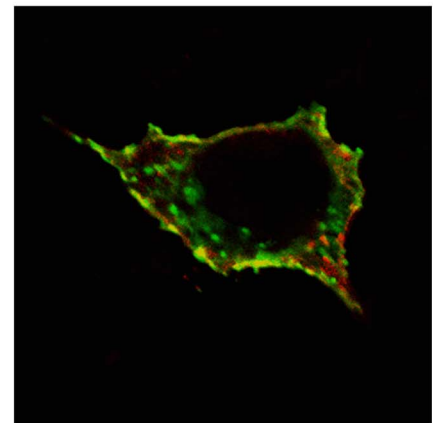
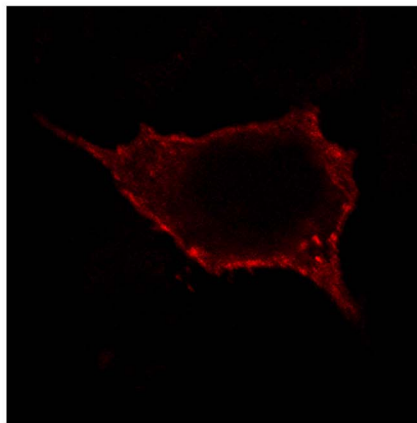
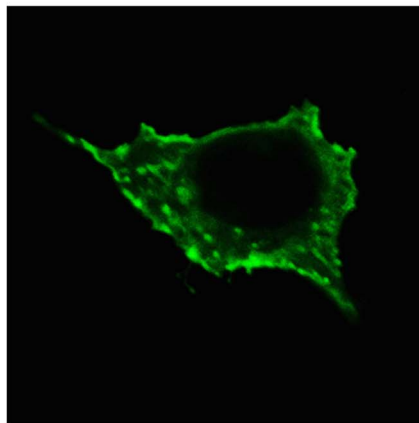


Figure 2. Visualization of β_2 AR and IR cellular localization by confocal microscopy. IR-GFP² and HA- β_2 AR-RLuc8 cellular localization is shown in untreated (control) cells (upper panels) and cells concomitantly treated with isoproterenol (10 μ M) and insulin (0.1 μ M) for 10 min at 37°C (lower panels). The green color indicates IR-GFP²; red indicates HA- β_2 AR-RLuc8; yellow/orange is the overlapping region indicating colocalization of IR-GFP² and HA- β_2 AR-RLuc8. Note that both receptors have comparable localization in untreated and agonist-stimulated cells and that they exhibit a high degree of colocalization. However, in agonist-stimulated cells a proportion of intracellular receptors did not colocalize. Objective 40 \times and zoom factor 4 apply for all images.

doi:10.1371/journal.pone.0112664.g002

then mounted using an anti-fading ProLong Gold reagent (Molecular Probes, the Netherlands), sealed and examined under an oil immersion objective (Planapo 40 \times , N.A. = 1.25) using a Leica multispectral confocal laser microscope (Leica TCS NT, Heidelberg, Germany). The sequential detection of GFP²- and TRITC-stained receptors was achieved using excitation laser lines at 488 nm (argon) and 543 nm (helium-neon), respectively. The fluorescence from the channels was collected sequentially, and images were produced using an 8-fold frame averaging a resolution of 1024 \times 1024 pixels. Optical sections (1.0 μ m) were acquired, and representative sections corresponding to the middle of the cells were presented using Adobe Photoshop 7.0 computer software.

BRET² saturation and competition assays

To derive BRET² saturation curves, HEK-293 cells were transiently cotransfected with constant amounts of the constructs encoding RLuc8-tagged receptors together with increasing amounts of the constructs encoding GFP²-tagged receptors. For

BRET² competition assays, HEK-293 cells were cotransfected with constant amounts of RLuc8- and GFP²-tagged receptor constructs and with increasing amounts of untagged receptors. BRET² assays were performed as described previously [24,46,47]. Briefly, 180 μ l of resuspended cells containing $\sim 2 \times 10^5$ cells was distributed in 96-well microplates (white Optiplate; Packard BioScience, Meriden, CT, USA). After the addition of coelenterazine 400a to a final concentration of 5 μ M using an injector, readings were collected (TriStar LB 942 microplate reader, Berthold Technologies, Bad Wildbad, Germany). Signals at 410 nm (RLuc8 luminescence signal) and 515 nm (emission of light from excited GFP²) were measured sequentially, and 515/410 ratios (BRET² signal) were calculated. The results were expressed in milliBRET units (mBU); BRET ratio \times 1000. The expression levels of RLuc8- and GFP²-tagged constructs for each experiment were assessed by total luminescence and fluorescence measurements as described above. Determinations were made in triplicates.

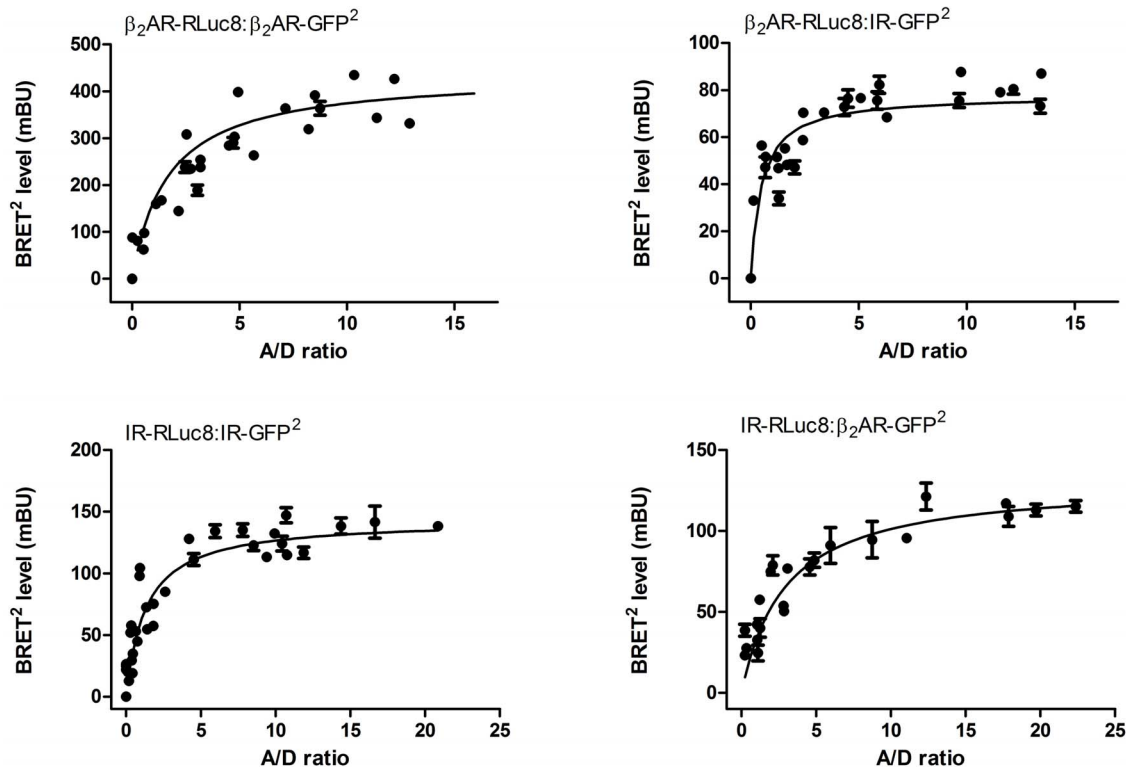


Figure 3. BRET² saturation curves of β_2 AR and IR homo- and heteromers. HEK-293 cells were transiently cotransfected with a constant amount of RLuc8-tagged and increasing amounts of GFP²-tagged receptor encoding constructs. BRET² values were plotted as a function of the ratio between the acceptor and donor fusion proteins (A/D ratio). A dataset is composed of 3–5 independent saturation experiments that were fitted using a nonlinear regression equation assuming a single binding site using GraphPad Prism 5.0 (Fitting results are found in Table 3). doi:10.1371/journal.pone.0112664.g003

BRET² assay data evaluation

The BRET² values were fitted using the following equation for dimers: $BRET = BRET_{max} / (1 + AD_{50}/X)$, where X is the ratio of acceptor (A; Receptor-GFP²) to donor (D; Receptor-RLuc8) molecules. $BRET_{max}$ is the maximum BRET² signal when all of the donor molecules are interacting with acceptor molecules. AD_{50} value corresponds to the acceptor/donor ratio providing 50% of the $BRET_{max}$ and reflects the relative affinity of the acceptor (GFP²-tagged receptor) for the donor molecules (RLuc8-tagged receptor). Fitting parameters were compared using Welch's t-test.

Simplistic BRET model for trimers with different association affinities

The BRET model for trimers is based on the Veacht and Steyer (1977) concept [50]. The theoretical saturation curve for trimers with the same association affinity is:

$$BRET = \frac{I_{acceptor}}{I_{donor}} = \frac{2EAAD + 2EADD}{(1-2E)AAD + 2(1-E)ADD + DDD} \quad (1)$$

where A, D and E are acceptor, donor and energy transfer efficiency, respectively. If we have different affinities for the formation of AAD trimer we introduce enhancement factor X:

$$BRET = \frac{I_{acceptor}}{I_{donor}} = \frac{2EXAAD + 2EADD}{(1-2E)XAAD + 2(1-E)ADD + DDD} \quad (2)$$

BRET competition assay simulation for trimers with different energy transfer ratio

The BRET model for trimer competition is based on the Veacht and Steyer (1977) concept [50]. For receptors with equal affinities to form trimers we determine the frequency of each trimer type (A = acceptor, D = donor and W = wild type receptor):

$$(A * D * W)^3 = AAA + 3AAD + 3AAW + 3ADD + 6ADW + 3AWW + 3DDW + 3DWW + DDD + WWW \quad (3)$$

BRET is defined as a ratio of light emission from acceptor divided by that of the donor. E is resonance energy transfer ratio:

$$BRET = \frac{I_{acceptor}}{I_{donor}} = \frac{2EAAD + 2EADD + 2EADW}{(1-2E)AAD + 2(1-E)ADD + 2(1-E)ADW + 2DDW + DWW + DDD} \quad (4)$$

If the energy transfer ratio E is different for ADW trimers the following equation is obtained:

$$BRET = \frac{I_{\text{acceptor}}}{I_{\text{donor}}} = \frac{2E_1AAD + 2E_1ADD + 2E_2ADW}{(1 - 2E_1)AAD + 2(1 - E_1)ADD + 2(1 - E_2)ADW + 2DDW + DWW + DDD} \quad (5)$$

Informational spectrum method (ISM)

The ISM is based on a model that assigns to each amino acid a defined parameter describing a physico-chemical property involved in the biological activity of the protein and corresponding to electron-ion interaction potential (EIIP). These values determine the electronic properties of the amino acids responsible for their intermolecular interactions [51].

The obtained numerical sequence, representing the primary structure of a protein, is then subjected to a discrete Fourier transformation defined as follows:

$$X(n) = \sum x(m)e^{-j(2/N)nm}, n = 1, 2, \dots, N/2 \quad (6)$$

where $x(m)$ is the m -th member of a given numerical series, N is the total number of points in this series, and $X(n)$ are discrete Fourier transformation coefficients. These coefficients describe the amplitude, phase and frequency of sinusoids, which comprised the original signal. The absolute value of the complex discrete Fourier transformation defines the amplitude spectrum and phase spectrum. The complete information concerning the original sequence is contained in both spectral functions. However, in the case of protein analysis, relevant information is presented in an energy density spectrum (for a review, see [51]) defined as follows:

$$S(n) = X(n)X^*(n) = 1/2X(n)1/2^2, n = 1, 2, \dots, N/2. \quad (7)$$

Thus, the initial information defined by the sequence of amino acids is now presented in the form of the informational spectrum (IS), representing the series of frequencies and their amplitudes.

The IS frequencies correspond to the distribution of structural motifs with defined physico-chemical characteristics responsible for the biological function of a protein. When comparing proteins that share the same biological or biochemical function, ISM allows the detection of code/frequency pairs that are specific for their common biological properties or correlate with their specific interaction. This common informational characteristic of sequences is determined by a cross-spectrum (CS) for two proteins or consensus informational spectrum (CIS) for two or more proteins—

i.e., the Fourier transformation of the correlation function for the spectrum. In this way, any spectral component (frequency) not present in all of the compared ISs is eliminated. Peak frequencies in CIS are common frequency components for the analyzed sequences. A measure of similarity for each peak is the signal-to-noise ratio (S/N), representing the ratio between the signal intensity at one particular IS frequency and the main value of the whole spectrum. If a CIS is calculated for a group of proteins with different primary structures, and strictly defined peak frequencies are found, the analyzed proteins likely participate in a mutual interaction or have a common biological function. The ISM was, thus far, successfully applied in the structure-function analysis of different protein sequences [51], prediction of new protein interactors [43] and identification of protein domains responsible for long-range interactions [52,53].

Computational peptide scanning

Computational peptide scanning was used to define linear protein regions that contribute the most to the amplitude and signal to noise ratio at the characteristic frequency and, therefore, are responsible for the interaction(s) described by the particular spectral characteristic. To identify the regions with the highest amplitudes at predefined Fourier frequencies, the entire sequences of β_2 AR and IR were scanned by the ISM algorithm with overlapping windows of different lengths, leading to the identification of regions with the highest amplitudes at predefined Fourier frequencies.

Datasets

The sequences used for bioinformatics analysis were retrieved from the Uniprot database with the following accession numbers: P07550 (human β_2 AR) and P06213 (human IR isoform A that lacks exon 11).

Statistical analysis

Statistical significance was determined using Student's t-test and Welch's t-test. Differences were considered statistically significant at a p value less than 0.05.

Ethics Statement

N/A.

Results

Characteristics of the β_2 AR fusion constructs

Pharmacological characterization of the human HA-tagged β_2 AR (HA- β_2 AR) fused at the C-terminus with either the energy donor RLuc8 or energy acceptor GFP² was performed using

Table 3. BRET² saturation assay fitting results.

Receptor pair	BRET _{max} (mBU)	AD ₅₀
β_2 AR-RLuc8: β_2 AR-GFP ²	437 ± 35	1.7 ± 0.5
IR-RLuc8:IR-GFP ²	143 ± 10	1.3 ± 0.4
β_2 AR-RLuc8:IR-GFP ²	78 ± 4	0.5 ± 0.1
IR-RLuc8: β_2 AR-GFP ²	131 ± 11	2.9 ± 0.7

BRET² data from saturation assays were fitted using the following equation for dimers: $BRET = BRET_{\text{max}}(1/(1 + AD_{50}/X))$ where X is the ratio of acceptor (A; Receptor-GFP²) to donor (D; Receptor-RLuc8) molecules. The BRET_{max} is the maximal BRET obtained for a given pair and AD₅₀ value corresponds to the A/D ratio providing 50% of the BRET_{max}. The best-fit parameters and standard errors were derived from the data presented in Fig. 3. Fitting parameters were compared using Welch's t-test. Statistical analysis shows that AD₅₀ and BRET_{max} values differ significantly ($p \leq 0.05$) between all of the tests.

doi:10.1371/journal.pone.0112664.t003

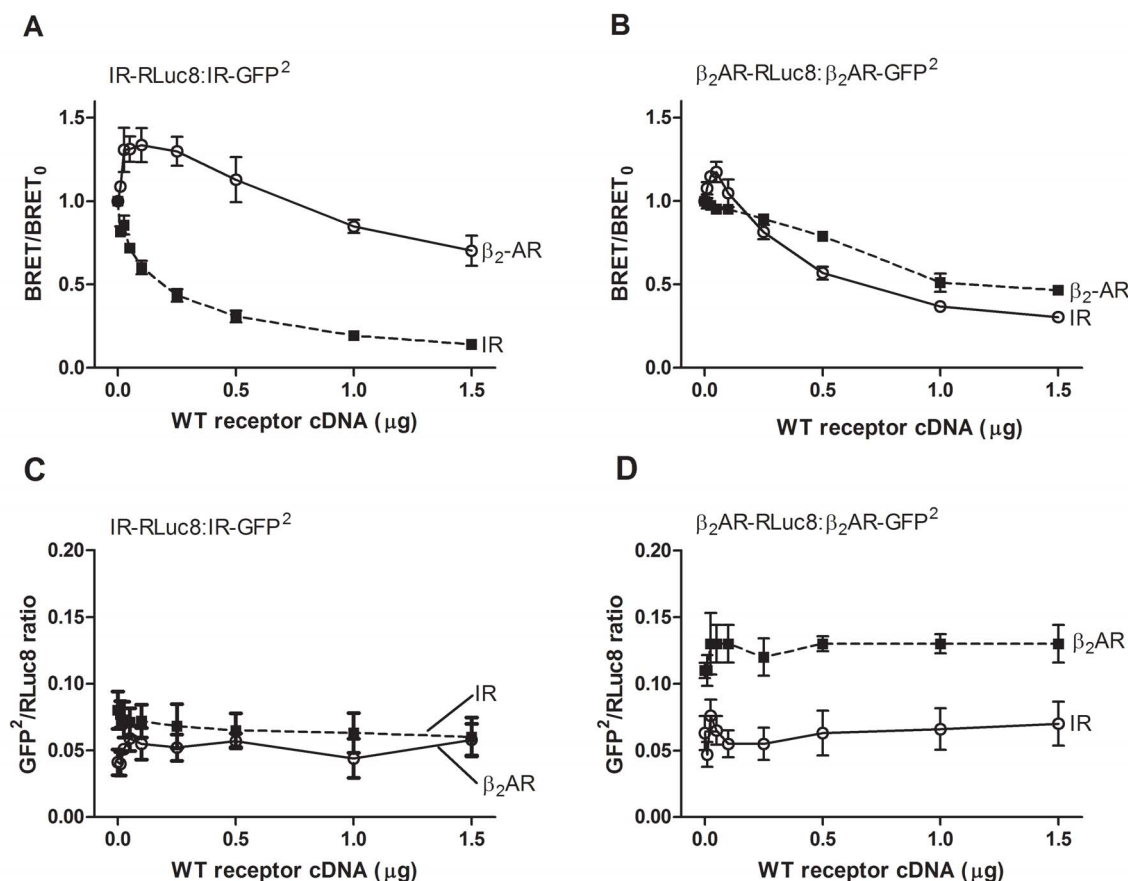


Figure 4. Homologous and heterologous BRET² competition assay. (A, B) HEK-293 cells were cotransfected with a constant amount of RLuc8- and GFP²-tagged receptor while increasing the amount of untagged receptor. In the homologous competition assay (dotted line), BRET² signals decreased with an increasing amount of WT receptor confirming the competition effect. In the heterologous BRET² assay (solid line), where different WT receptors were used to compete with the tagged homomer receptor pair, a transient increase in the BRET² signal with a subsequent hyperbolic decrease was observed. BRET₀ is the BRET² signal obtained in the absence of competitor. Data are expressed as the means \pm S.E. from three independent experiments performed in triplicate. (C, D) Receptor-GFP²/Receptor-RLuc8 expression ratio (GFP²/RLuc8 ratio) in each sample was evaluated for total luminescence and total fluorescence. Total luminescence and total fluorescence was measured as described under Material and Methods. Note that GFP²/RLuc8 ratio was roughly constant in the absence or presence of increasing concentrations of competitor (untagged β₂AR or IR). Data are expressed as the means \pm S.E. from three independent experiments performed in triplicate.
doi:10.1371/journal.pone.0112664.g004

radioligand binding assays (Table 1). The IC₅₀ values of pindolol for HA-β₂AR-RLuc8 and β₂AR-GFP² were in agreement with those obtained for HA-β₂AR and were also in the range previously

reported for β₂AR-RLuc fusion construct [47]. IR fusion constructs were previously characterized [34]. Radioligand binding assays were also performed with HEK-293 cells cotransfected

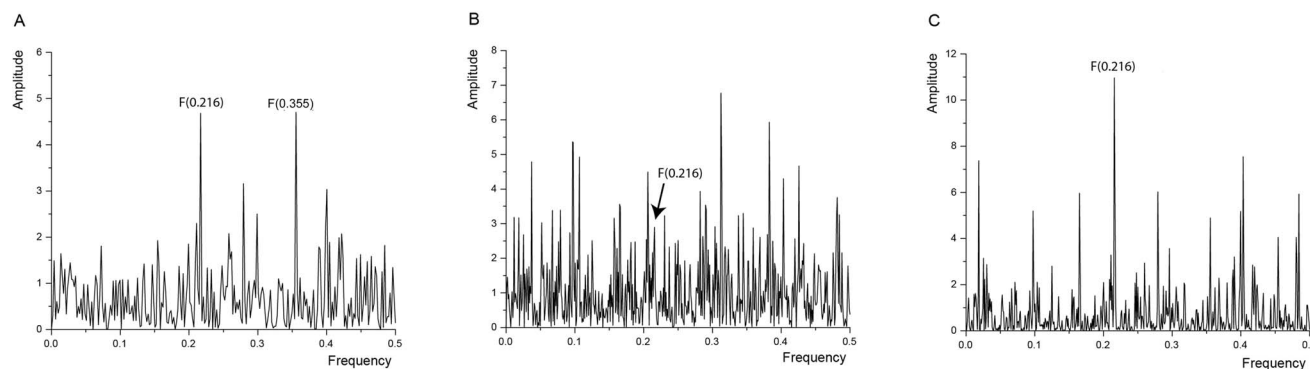


Figure 5. Informational spectrum (IS) of (A) β₂AR, (B) IR and (C) cross-spectrum (CS) of β₂AR and IR. CS of β₂AR and IR revealed common information corresponding to the IS frequency F(0.216) (panel C).
doi:10.1371/journal.pone.0112664.g005

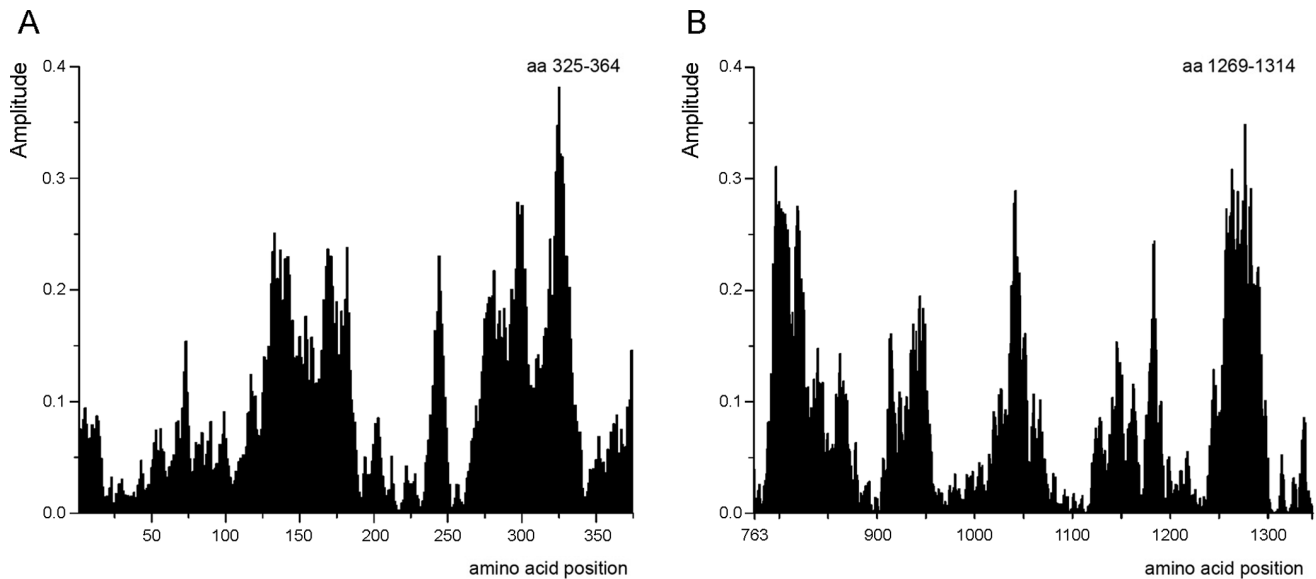


Figure 6. Mapping of the domains with maximal contribution to the frequency component F(0.216) in the informational spectrum of (A) β_2 AR and (B) IR. Peptide scanning of the β_2 AR and IR identified regions encompassing residues at the end of the 7th TM domain and C-terminal tail of β_2 AR and 1269–1314 IR (B) are essential for the information represented by the frequency F(0.216). The position of the first amino acid (aa) in the domain is shown. Panel B; the amino acid position denote the positions in IR β subunit starting from amino acid 763.
doi:10.1371/journal.pone.0112664.g006

with the HA- β_2 AR and IR at a 1:1 cDNA ratio. The obtained IC_{50} values for the tested β_2 AR ligands—i.e., pindolol and isoproterenol—were comparable in β_2 AR- and in β_2 AR- and IR-expressing cells. Similarly, heteromerization with β_3 AR did not affect the binding properties of β_2 AR [20]. Insulin neither competed for binding against [¹²⁵I]-iodopindolol nor affected the IC_{50} values of pindolol (Table 2).

β_2 AR surface expression and the internalization effect of IR coexpression

The effect of IR coexpression on β_2 AR surface expression and internalization properties was evaluated by ELISA in intact cells and by radioligand binding assays. As shown in Fig. 1A, a significant approximately 35% decrease in β_2 AR surface expression was observed in HEK-293 cells cotransfected with IR compared with β_2 AR-expressing cells ($p < 0.05$). However, total

β_2 AR expression was not affected by IR coexpression as shown by luminescence measurements, whereas IR expression was validated by fluorescence measurements. Analogous observations in β_2 AR surface expression were detected using radioligand binding assays, where β_2 AR surface expression decreased by around 30% (27.89 ± 2.11) in HEK-293 cells cotransfected with IR compared with β_2 AR-expressing cells ($p < 0.05$).

Additionally, ELISA measurements suggested that IR coexpression moderately increased isoproterenol-induced β_2 AR internalization, whereas concomitant treatment with isoproterenol and insulin evoked a comparable internalization rate. Treatment with insulin did not induce marked β_2 AR internalization (Figure S1). To further examine the internalization kinetics of β_2 AR, HEK-293 cells expressing either β_2 AR or β_2 AR and IR were treated with either isoproterenol (10 μ M) or a combination of both isoproterenol (10 μ M) and insulin (0.1 μ M) for varying periods of

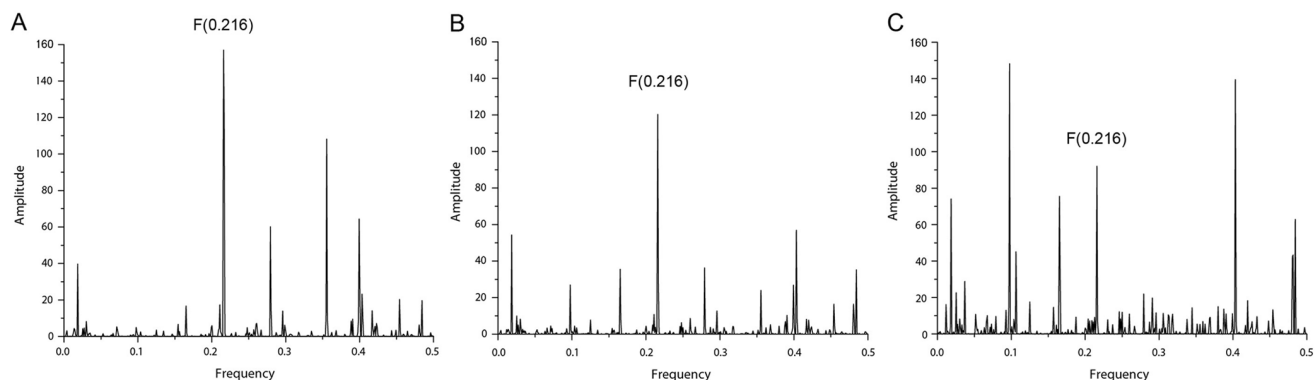


Figure 7. Consensus informational spectrum (CIS) of β_2 AR:IR tetramers with the characteristic peak at F(0.216). (A) β_2 AR: β_2 AR: β_2 AR:IR, (B) β_2 AR: β_2 AR:IR:IR and (C) β_2 AR:IR:IR:IR tetramers. Note that the interaction affinities among the receptors decreased in the order β_2 AR: β_2 AR: β_2 AR:IR \geq β_2 AR: β_2 AR:IR:IR $>$ β_2 AR:IR:IR:IR.
doi:10.1371/journal.pone.0112664.g007

time (5 min to 1 h), and the number of cell surface binding sites were determined (Fig. 1B and C). We found that isoproterenol-induced steady-state proportion of internalized receptors was approximately 38% and 44% in β_2 AR- and in β_2 AR- and IR-expressing cells, respectively. The rate of isoproterenol-induced β_2 AR internalization was significantly increased by coexpression of IR ($p < 0.05$), as the estimated $t_{1/2}$ was 8.6 ± 1.3 and 5.4 ± 0.6 min in β_2 AR- and in β_2 AR- and IR-expressing cells. Comparable results were obtained when either β_2 AR- or β_2 AR- and IR-expressing cells were concomitantly treated with isoproterenol and insulin (see Fig. 1B and C). In addition, confocal fluorescence microscopy demonstrated predominant plasma membrane localization of the HA- β_2 AR-RLuc8 and IR-GFP² and their colocalization in untreated cells (Fig. 2, upper panels; untreated cells). Concomitant treatment of β_2 AR- and IR-expressing cells with isoproterenol and insulin (Fig. 2, lower panels) promoted receptor redistribution to the cytoplasm, indicating receptor internalization. Again, agonist-redistributed β_2 AR and IR showed a similar distribution pattern; however, a proportion of intracellular receptors did not colocalize.

Interaction between the β_2 AR and IR-BRET evidence

Considering the observed effects of IR coexpression on β_2 AR surface expression and internalization, as well as colocalization of both receptors in HEK-293 cells, we next investigated whether proximity indicative of direct interaction occurs between β_2 AR and IR by performing BRET dilution, saturation and competition assays. To obtain an absolute value of donor [D] and acceptor [A] molecules—i.e., Receptor-RLuc8 and Receptor-GFP²—we first generated correlation curves between total luminescence and fluorescence *versus* the number of receptor-binding sites determined by radioligand binding. The linear correlation was obtained between the number of HA- β_2 AR-RLuc8 and β_2 AR-GFP² binding sites and the total luminescence and total fluorescence, respectively (Figure S2).

The derived correlation factors to convert total luminescence and total fluorescence into receptor number were 0.00031 and 0.0089, respectively. Thereafter, BRET² dilution assays with a constant $[A]/[D]$ ratio were performed to set the concentration

range for the saturation assays and distinguish monomers from dimers as previously described [54]. Due to the increasing noise in calculated BRET at low luminescence intensities, the lowest amount of HA- β_2 AR-RLuc8 and IR-RLuc8 cDNA used for transfection in saturation assays was determined at 0.05 and 0.015 μ g, respectively.

BRET² saturation assays were performed to investigate homo- and hetero-merization of β_2 AR and IR. The BRET² signal was measured in live HEK-293 cells that were transiently transfected with constant amounts of RLuc8-tagged (HA- β_2 AR-RLuc8, IR-RLuc8) and with increasing amounts of GFP²-tagged (β_2 AR-GFP², IR-GFP²) receptor encoding constructs. In dimers and higher oligomers, the probability of BRET interaction increases with increasing acceptor/donor ratio until all of the acceptors have pairs, and the maximum BRET² level (BRET_{max}) or plateau is reached. The AD₅₀ value (also designated as BRET₅₀; see methods) was also included to compare the affinity for homo- / heteromer formation. BRET² saturation experiments data are shown in Fig. 3 and the expression levels of RLuc8- and GFP²-tagged receptor constructs are shown in Figure S3. For all of the receptor combinations, the BRET² signal was plotted as a function of the A/D ratio increased as a hyperbolic function reaching a saturation level (Fig. 3). Control experiments for the specificity of the interaction were performed by cotransfecting RLuc8-tagged receptors with increasing amounts of membrane-inserted GFP²-tagged construct (GFP²-17aa). Plasma membrane localization of the GFP²-17aa construct was previously demonstrated [45]. The BRET² signal increased linearly with the increase in fluorescence/ luminescence (GFP²/RLuc8) ratio, most likely reflecting random collisions between the RLuc8-tagged receptors and control unrelated GFP²-tagged construct (GFP²-17aa) (Figure S4). Saturation assay data were fitted using a dimer model in the approximation of small energy transfer [54] (Table 3). We observed the highest BRET_{max}—i.e., 437 mBU in the β_2 AR homologous saturation assay and considerably lower BRET_{max} values for other receptor combinations. It should be stressed that the BRET_{max} value depends on the distance between BRET pairs and is not a measure of the strength of interaction between the acceptor- and donor-tagged receptors. In homologous saturation

Table 4. The affinity of interaction between the β_2 AR and IR homo- and heteromers characterized by the signal-to-noise ratio (S/N) at the characteristic frequency (F) in the consensus informational spectrum (CIS).

Dimer	S/N ratio
β_2 AR: β_2 AR	24.082
β_2 AR:IR	15.951
IR:IR	22.407
Trimer	
β_2 AR: β_2 AR: β_2 AR	52.867
β_2 AR: β_2 AR:IR	43.476
β_2 AR:IR:IR	25.605
IR:IR:IR	51.146
Tetramer	
β_2 AR: β_2 AR: β_2 AR: β_2 AR	81.703
β_2 AR: β_2 AR: β_2 AR:IR	76.505
β_2 AR: β_2 AR:IR:IR	71.105
β_2 AR:IR:IR:IR	29.468
IR:IR:IR:IR	89.617

doi:10.1371/journal.pone.0112664.t004

assays, the value of AD_{50} for the IR homomer was significantly lower ($p \leq 0.05$) than that for the β_2 AR homomer (Table 3). For the receptor complex consisting of β_2 AR-RLuc8:IR-GFP², the AD_{50} value was significantly lower ($p \leq 0.05$) than the AD_{50} value for the IR-RLuc8: β_2 AR-GFP². For heterodimers, there should be no difference in the relative affinity between AD and DA dimers. To interpret our data, we developed a simplistic trimer model for interpretation of AD_{50} values in a BRET saturation assay. According to this model, different AD_{50} values are derived from theoretical BRET saturation curves with different affinities for various types of trimer formation (Figure S5). This model should be used with caution because it does not take into account the simultaneous formation of dimers, trimers and higher-order oligomers. Stimulation with the agonists insulin or isoproterenol did not promote any detectable change in the BRET² signal (data not shown), indicating that the receptor dimers/oligomers form constitutively and that addition of agonists does not induce a detectable change in the conformational or oligomerization state of the receptor complexes. However, it needs to be stressed that BRET only provides information concerning a steady-state population of dimer/higher-order oligomers and is not suited to monitor the rapid, “real-time” dynamic type of di-/oligomerization [55].

To further support the findings from the saturation assays, we performed homologous and heterologous BRET² competition assays where HEK-293 cells were co-transfected with a constant amount of RLuc8- and GFP²-tagged receptor while increasing the amount of untagged receptor (Fig. 4A and B). Competition experiments were carried out at the constant Receptor-GFP²/Receptor-RLuc8 expression ratio to avoid possible variations in the BRET² signal due to fluctuation in the relative expression levels of the energy donor and acceptor (Fig. 4C and D). It is expected that the BRET² signal would decrease if untagged receptors compete with the tagged receptors for the binding in complexes. In homologous BRET² competition assays BRET² signal decreased with increasing amount of competitor (un-tagged receptor). In the IR homologous competition assay, we observed a typical competition curve for dimers, where introduction of the same amount of untagged receptor produced an approximately 50% reduction in the observed BRET signal. In the β_2 AR homologous competition assay, the reduction of the BRET signal was smaller. This observation cannot be explained by a simple dimer or trimer model; it could be attributed to clustering of the β_2 AR where several acceptors can interact with each donor. In heterologous competition assays, we observed a transient increase in the BRET signal with a later hyperbolic decrease (see Fig. 4A and B). Untagged β_2 AR caused approximately 1.4-fold increase in the IR BRET signal, while the effect of untagged IR on the β_2 AR BRET signal was less obvious; maximal observed increase was less than 1.2-fold. The transient increase in the BRET signal with a subsequent hyperbolic decrease is theoretically predicted for trimers or higher-order oligomers, where the donor, acceptor and competitor are all present in the same complex (Figure S6).

Interaction between β_2 AR and IR characterized by ISM

To support our experimental evidence with the bioinformatics data, we next applied the informational spectrum method (ISM), a virtual spectroscopy method to investigate protein-protein interactions and to analyze the structure/function relationship of proteins. ISM was utilized to identify important informational characteristic of the interaction between β_2 AR and IR and identify the structural determinants potentially involved in receptor heteromerization. The primary structure of proteins encodes the information represented by the informational spectrum (IS)

frequencies that correspond to the protein biological function. Mutually interacting proteins share common information that is represented by peaks in their cross-spectrum [51]. The informational spectrum of β_2 AR is presented in Fig. 5A. It contains two characteristic peaks at the frequency F(0.216) and F(0.355). Fig. 5B represents the IS of the IR. By performing cross-spectral analysis of β_2 AR and IR, we have identified that these two molecules share common information corresponding to the IS frequency F(0.216) (Fig. 5C). To further evaluate the importance of the peak at F(0.216) we performed CS analysis of β_2 AR and IR with scrambled IR and β_2 AR proteins as negative controls. The scrambled proteins with the identical amino acid composition to that of β_2 AR and IR were created by random permutation of original proteins. CS analysis between wild type receptors and randomly selected scrambled β_2 AR and IR are presented in Figure S7. The intensity of whole spectrum and the value of amplitudes at the characteristic peak F(0.216) is higher in CS of two wild type proteins compared to CS of original and scrambled proteins confirming the importance of the characteristic peak at the F(0.216) for interaction between β_2 AR and IR.

Identification of the key protein domains responsible for the interaction between β_2 AR and IR

Computational peptide scanning of β_2 AR and IR was performed to identify the regions of proteins essential for information corresponding to the frequency F(0.216). The computer-assisted peptide scanning survey of the primary structure of β_2 AR with overlapping windows of different lengths revealed that the region encompassing residues 325–364 is essential for the information represented by the frequency F(0.216) (Fig. 6A). Further peptide scanning of IR identified three principal regions as important for the information represented by the frequency F(0.216), however region encompassing residues 1269–1314 represents the most probable domain involved in this interaction (Fig. 6B).

Affinity of interaction between protomers

Peak frequencies in CIS represent common information encoded by the primary structures of analyzed proteins. Significance of information is determined by the signal-to-noise ratio (S/N), representing the ratio between the signal intensity at one particular IS frequency and main value of the whole spectrum. A higher S/N value at the characteristic frequency (F) in CS/CIS of two or more proteins suggests a higher propensity for their interaction.

The current analysis showed that the interaction affinities between the homomers of β_2 AR and IR are similar and that at the level of dimer formation, both β_2 AR and IR displayed a higher propensity toward homodimerization than heterodimerization (Table 4). Considering that in the CS of the β_2 AR and IR, the two receptors share common information corresponding to the IS frequency F(0.216), it can be assumed that this frequency is equally important for heterodimerization and for higher-order hetero-oligomer formation. The obtained S/N values at F(0.216) in the CS of β_2 AR: β_2 AR: β_2 AR:IR and β_2 AR: β_2 AR:IR:IR tetramers were comparable, whereas that for the IR trimer displayed a considerably lower affinity for interaction with the β_2 AR monomer (Fig. 7 and Table 4).

Discussion

7TMRs form the largest and most important pharmacotherapeutic target in drug discovery. Continual discovery of receptor heteromers expands the repertoire of functional 7TMR units and

offers promising new targets for drug development (reviewed in [56]). Increasing evidence for the existence of functional 7TMR:RTK heteromers [7,36,37,38,39] adds another level of complexity to this system. In the present study, we combined *in vitro* experimental and bioinformatics approaches for the investigation of the interaction between β_2 AR and IR. Initially, it was observed that IR coexpression reduces β_2 AR surface expression and accelerates its internalization. It could be assumed that IR increased constitutive internalization of the β_2 AR [57], thereby reducing its surface expression. The extent of isoproterenol-induced β_2 AR internalization was comparable to the previously reported internalization rate for β_2 AR [58,59]. The estimated $t_{1/2}$ of ~ 9 min for isoproterenol-induced β_2 AR internalization is also within the range reported for the same receptor using a fluorimetric assay [60]. Augmented agonist-induced β_2 AR internalization promoted by IR coexpression is in good agreement with that described in a previous report [61]. The amount of surface-expressed β_2 AR lost to internalization in response to insulin in HEK-293, $\sim 15\%$, correlated well with results obtained in DT₁MF-2 smooth muscle cells and CHO cells [61,62] but was smaller than the reported value of $\sim 30\%$ in epidermoid carcinoma A431 cells [6]. Our colocalization results in untreated cells correlate well with recent coimmunoprecipitation findings demonstrating that β_2 AR and IR form complexes in the mouse heart, in which the stimulation of IR resulted in the reduction of the association of the β_2 AR:IR complex [7].

BRET results provided further evidence for the direct interaction between β_2 AR and IR. Hyperbolic saturation assay curves are indicative of a specific constitutive interaction between IR and β_2 AR. The BRET_{max} obtained for β_2 AR homomerization is higher than that described in previous reports [19,23,24], whereas the relative affinity of β_2 AR for homomerization is within the previously reported range (AD_{50} of 1.7 ± 0.5 vs. 1.2 ± 0.33 [23]). The RLuc8/GFP² BRET² donor/acceptor pair used in our study has the largest Förster distance R_0 , leading to 50% of energy transfer from the donor to acceptor, thereby extending the maximum distance that the BRET² system can accurately measure [63]. Lower reported BRET_{max} values were obtained with original BRET¹ [19] or BRET² [23,24] combinations. The BRET_{max} values generated in the homologous IR saturation assay were also slightly higher than that previously reported [29]. The same study revealed that the substantial insulin-induced effect on the BRET signal could only be detected with partially purified fusion IRs [29]. Single-molecule analysis of fluorescently labeled 7TMRs recently demonstrated that β_2 AR had a high tendency of forming dimers, even at low densities comparable to receptor expression in native tissue; however, at higher densities, β_2 AR formed a mixture of di-, tri-, and tetramers [55]. Membrane-driven spatial organization of β_2 AR also favors its stable/extensive oligomerization [64]. The inability of agonists to modify the oligomerization status of β_2 AR was also reported in studies that utilized methods other than BRET (reviewed by Ferre et al. [56]). Both receptors displayed a similar propensity to form homomers as assessed by AD_{50} and S/N values. Affinities for the formation of β_2 AR:IR and IR: β_2 AR heteromers differed substantially, a finding that could not be explained by a dimer model that assumed a heteromer stoichiometry of 1:1. The lower AD_{50} value observed for the β_2 AR-RLuc8:IR-GFP² pair could suggest either a higher affinity for heteromer formation or, alternatively, complex oligomer formation. The melatonin MT₂ receptor also displayed a higher propensity for heteromerization with the MT₁ receptor [65], whereas certain receptor pairs (i.e., β_1 AR: β_2 AR [23,24], β_2 AR: β_3 AR [20]), oxytocin and vasopressin receptors [66] showed a similar propensity, and muscarinic acetylcholine receptors [67]

showed a slightly lower propensity for heteromerization. However, simplistic model for interpretation of AD_{50} values and heterologous competition assays data provided evidence for higher-order oligomeric complex formation. A transient increase in the BRET signal suggests that the energy transfer efficiency E is increased in hetero-oligomeric complexes due to the smaller distance between the BRET donor/acceptor pair in the complex (see Figure S6). A similar effect—i.e., an increased homo-dimer BRET signal induced by an unrelated, untagged receptor—was previously observed with the gastric inhibitory polypeptide receptor [24]. Therefore, both the change in affinities and transient increase in the BRET signal could be a reflection of higher-order oligomeric complexes with affinities for distinct associations such as with trimers and tetramers with 2:1 and 2:2 stoichiometry, respectively, as proposed by Breitwieser et al. [68]. At the level of dimer formation, both β_2 AR and IR displayed a higher propensity toward homodimerization than heterodimerization, suggesting homodimers as the basic units engaged in heteromerization. Affinity calculation for trimers and tetramers highlighted differences between β_2 AR and IR. Apparently, neither IR dimers nor trimers could form high affinity interactions with the β_2 AR monomer. However, IR monomers/homodimers can form high affinity heteromers with β_2 AR di-/trimers. Considering that both receptors displayed a higher propensity toward homodimerization and that IR is present in the plasma membrane as a disulfide-linked dimer [28], it is plausible to suggest that high-order 7TMR:RTK oligomers most likely comprise heteromers of homodimers (2:2 stoichiometry). The computer-assisted peptide scanning survey of the primary structure of β_2 AR and IR revealed the domain encompassing residues 325–364 and 1269–1314 as prospective interaction domains. The identified region is located at the end of the 7th TM domain and C-terminal tail of β_2 AR and almost completely overlaps with helix 8 (helix adjacent to TM7 running along the internal membrane surface) of β_2 AR (residues L324–N357) [69]. A recent study also identified β_2 AR helix 8 as an important dimerization surface region [70]. In addition, this region contains major sites (Tyr350/Tyr354 and Tyr364) for IR-mediated phosphorylation of β_2 AR [3,71] and consensus sites of Akt-catalyzed phosphorylation (Ser345/Ser 346) [72]. These results are in accordance with previous findings showing that β_2 AR is a substrate for IR and proposing direct interaction between these proteins [3,71]. The C-terminal cytoplasmic tail—more specifically, the 15-amino acid motif (residues 342–356)—was sufficient to confer the β_1 AR- β_2 AR tail chimera the ability to be regulated by insulin [62].

The prospective interaction domain identified in IR (residues 1269–1314) is positioned in the cytoplasmic part of the IR β chain. This region encompasses the terminal end of the tyrosine kinase catalytic domain and is a part of the C-terminal tail. The C-terminal domain of the IR β subunit has been found to play a key role in the regulation of tyrosine kinase activity [73,74]. The construct based on proteolytic cleavage used to solve the crystal structure of the IR tyrosine kinase domain of the human IR B-isoform [75] ends at residue 1283, which corresponds to the amino acid at position 1271 in the human IR isoform A used in our study. Therefore, it could be hypothesized that the terminal end of the IR tyrosine kinase domain and a part of the C-terminal tail are involved in the interaction with β_2 AR.

The involvement of intracellular domains (C-terminal tail and ICL3) was found to be fundamental for heterodimerization between the cannabinoid CB₁ receptor, adenosine A_{2A} and dopamine D₂ receptors, thus favoring the idea that electrostatic interactions between intracellular domains are more predominant

in receptor heteromers and constitute a general mechanism for receptor heteromerization [76].

In summary, BRET data and ISM bioinformatics provided evidence for direct interaction and higher-order β_2 AR:IR oligomer formation that we hypothesize comprise heteromers of homodimers and identified prospective intracellular interaction domains engaged in heteromerization. In this regard, 7TMR:RTK heteromers could potentially generate a basis for the design of new therapeutics that can compete with today's epidemics, such as type-2 diabetes, obesity and cardiovascular diseases.

Supporting Information

Figure S1 HA- β_2 AR internalization as quantified by ELISA. Cells transiently transfected with HA- β_2 AR (open bars) or HA- β_2 AR together with IR (hatched bars) at a 1:1 cDNA ratio were incubated at 37°C with either isoproterenol (10 μ M), insulin (0.1 μ M) or combination of both ligands for 30 min. The amount of internalized receptor was then calculated from the decrease in the level of surface-expressed receptor after ligand treatment compared with untreated, control cells. Data are expressed as the means \pm S.E. from three independent experiments performed in triplicate.

(TIF)

Figure S2 Correlation between total luminescence and fluorescence and the corresponding number of β_2 AR binding sites. HEK-293 cells were transfected with increasing amounts of HA- β_2 AR-RLuc8 (A) or β_2 AR-GFP² (B) encoding constructs. The β_2 AR receptor density (B_{\max}) was determined by radioligand binding assays using [¹²⁵I]-iodopindolol as a tracer as described in the Material and methods section. Total luminescence was measured after the addition of the RLuc8 substrate coelenterazine 400a. Total fluorescence was measured with an excitation filter at 380 nm and an emission filter at 515 nm. The linear regression curves were generated using GraphPad Prism 5.0. R^2 fit values of 0.9705 and 0.9861 were obtained for HA- β_2 AR-RLuc8 (A) and β_2 AR-GFP² (B), respectively.

(TIF)

Figure S3 Relationship between receptor-RLuc8 and receptor-GFP² constructs expression. Expression levels of RLuc8- and GFP²-tagged constructs used in BRET² saturation assays were also monitored by luminescence and fluorescence measurements. Total luminescence was measured after the addition of the RLuc8 substrate coelenterazine 400a. Total fluorescence was measured with an excitation filter at 380 nm and an emission filter at 515 nm. Data are expressed as the means \pm S.E. of 3–5 independent saturation experiments.

(TIF)

Figure S4 Random collisions between the RLuc8-tagged receptors and membrane-inserted GFP²-tagged construct (GFP²-17aa). HEK-293 cells were transiently cotrans-

fected with a constant amount of RLuc8-tagged receptors and increasing amounts of GFP²-17aa encoding construct. BRET² values were plotted as a function of the ratio between the total fluorescence/total luminescence (GFP²/RLuc8 ratio). Total luminescence was measured after the addition of the RLuc8 substrate coelenterazine 400a. Total fluorescence was measured with an excitation filter at 380 nm and an emission filter at 515 nm. Increasing the concentration of GFP²-17aa in cells expressing either the IR-RLuc8 or β_2 AR-RLuc8 resulted in high, but nonspecific linear increase of the BRET² signal. Data are expressed as the means \pm S.E. from three independent experiments performed in triplicate. Representative BRET² saturation curves of β_2 AR and IR homomers are shown for comparison.

(TIF)

Figure S5 Comparison of theoretical BRET saturation curves with different affinities for trimer formation.

Shown are simulated BRET saturation curves for case with the same affinity for AAD and ADD formation (solid line) and two special cases with different affinities for formation of AAD compared to ADD (hatched and dotted lines). Note that in all three cases the AD_{50} values are different. A: acceptor; D: donor.

(TIF)

Figure S6 Numerical simulation of heterologous BRET competition assay for trimers.

Comparison of simulated BRET competition curves for trimers with the same ($E_1 = E_2 = 0.1$) and different ($E_1 = 0.1$, $E_2 = 0.3$) energy transfer ratios for ADD and ADW, where A, D and W are concentrations of acceptor ($A = 1$), donor ($D = 1$) and (W) wild type receptors i.e. competitor. Transient increase in BRET signal is observed in the case of different ($E_1 = 0.1$, $E_2 = 0.3$) energy transfer ratios (dotted line). $BRET_0$ is the BRET signal obtained in the absence of competitor.

(TIF)

Figure S7 Cross-spectrum (CS) of (A) wild type β_2 AR and IR, (B) scrambled β_2 AR and wild type IR and (C) scrambled IR and wild type β_2 AR.

Note that the value of amplitudes at the characteristic peak F(0.216) is higher in CS of two wild type proteins (panel A) compared to the CS of wild type and scrambled proteins (panels B and C).

(TIF)

Acknowledgments

The authors would like to thank Professor Pierre De Meyts for critical evaluation of the manuscript and American Journal Experts for proofreading the English usage in the manuscript.

Author Contributions

Conceived and designed the experiments: JN MV. Performed the experiments: MM. Analyzed the data: LD SG NV. Contributed reagents/materials/analysis tools: JN SG NV. Contributed to the writing of the manuscript: MM SG MV.

References

- Barnes PJ (2006) Receptor heterodimerization: a new level of cross-talk. *J Clin Invest* 116: 1210–1212.
- White MF, Kahn CR (1994) The insulin signaling system. *J Biol Chem* 269: 1–4.
- Baltensperger K, Karoor V, Paul H, Ruoho A, Czech MP, et al. (1996) The β -adrenergic receptor is a substrate for the insulin receptor tyrosine kinase. *J Biol Chem* 271: 1061–1064.
- Wang H, Doronin S, Malbon CC (2000) Insulin activation of mitogen-activated protein kinases Erk1,2 is amplified via β -adrenergic receptor expression and requires the integrity of the Tyr350 of the receptor. *J Biol Chem* 275: 36086–36093.
- Shih M, Malbon CC (1998) Serum and insulin induce a Grb2-dependent shift in agonist affinity of β -adrenergic receptors. *Cell Signal* 10: 575–582.
- Shumay E, Gavi S, Wang HY, Malbon CC (2004) Trafficking of β_2 -adrenergic receptors: insulin and β -agonists regulate internalization by distinct cytoskeletal pathways. *J Cell Sci* 117: 593–600.
- Fu Q, Xu B, Liu Y, Parikh D, Li J, et al. (2014) Insulin inhibits cardiac contractility by inducing a G_i-biased β_2 adrenergic signaling in hearts. *Diabetes* 63: 2676–2689.
- Heni M, Hennige AM, Peter A, Siegel-Axel D, Ordelheide AM, et al. (2011) Insulin promotes glycogen storage and cell proliferation in primary human astrocytes. *PLoS One* 6: e21594.

9. Lange LA, Norris JM, Langefeld CD, Nicklas BJ, Wagenknecht LE, et al. (2005) Association of adipose tissue deposition and beta-2 adrenergic receptor variants: the IRAS family study. *Int J Obes (Lond)* 29: 449–457.
10. Liggett SB, Shah SD, Cryer PE (1988) Characterization of beta-adrenergic receptors of human skeletal muscle obtained by needle biopsy. *Am J Physiol* 254: E795–E798.
11. Angers S, Salahpour A, Bouvier M (2002) Dimerization: an emerging concept for G protein-coupled receptor ontogeny and function. *Annu Rev Pharmacol Toxicol* 42: 409–435.
12. Lee SP, O'Dowd BF, George SR (2003) Homo- and hetero-oligomerization of G protein-coupled receptors. *Life Sci* 74: 173–180.
13. Achour L, Kamal M, Jockers R, Marullo S (2011) Using quantitative BRET to assess G protein-coupled receptor homo- and heterodimerization. *Methods Mol Biol* 756: 183–200.
14. Ayoub MA, Pileger KD (2010) Recent advances in bioluminescence resonance energy transfer technologies to study GPCR heteromerization. *Curr Opin Pharmacol* 10: 44–52.
15. Ferre S, Baler R, Bouvier M, Caron MG, Devi LA, et al. (2009) Building a new conceptual framework for receptor heteromers. *Nat Chem Biol* 5: 131–134.
16. Ferre S, Franco R (2010) Oligomerization of G-protein-coupled receptors: a reality. *Curr Opin Pharmacol* 10: 1–5.
17. Gurevich VV, Gurevich EV (2008) GPCR monomers and oligomers: it takes all kinds. *Trends Neurosci* 31: 74–81.
18. Palczewski K (2010) Oligomeric forms of G protein-coupled receptors (GPCRs). *Trends Biochem Sci* 35: 595–600.
19. Angers S, Salahpour A, Joly E, Hilairet S, Chelsky D, et al. (2000) Detection of β_2 -adrenergic receptor dimerization in living cells using bioluminescence resonance energy transfer (BRET). *Proc Natl Acad Sci U S A* 97: 3684–3689.
20. Breit A, Lagace M, Bouvier M (2004) Hetero-oligomerization between β_2 - and β_3 -adrenergic receptors generates a β -adrenergic signaling unit with distinct functional properties. *J Biol Chem* 279: 28756–28765.
21. Lavoie C, Mercier JF, Salahpour A, Umapathy D, Breit A, et al. (2002) β_1/β_2 -adrenergic receptor heterodimerization regulates β_2 -adrenergic receptor internalization and ERK signaling efficacy. *J Biol Chem* 277: 35402–35410.
22. McGraw DW, Muhlbacher KA, Schwab MR, Rahman FF, Small KM, et al. (2006) Airway smooth muscle prostaglandin-EP1 receptors directly modulate β_2 -adrenergic receptors within a unique heterodimeric complex. *J Clin Invest* 116: 1400–1409.
23. Mercier JF, Salahpour A, Angers S, Breit A, Bouvier M (2002) Quantitative assessment of β_1 - and β_2 -adrenergic receptor homo- and heterodimerization by bioluminescence resonance energy transfer. *J Biol Chem* 277: 44925–44931.
24. Vrecl M, Drinovec L, Elling C, Heding A (2006) Opsin oligomerization in a heterologous cell system. *J Recept Signal Transduct Res* 26: 505–526.
25. Wrzal PK, Devost D, Petrin D, Goupil E, Iorio-Morin C, et al. (2012) Allosteric interactions between the oxytocin receptor and the β_2 -adrenergic receptor in the modulation of ERK1/2 activation are mediated by heterodimerization. *Cell Signal* 24: 342–350.
26. Issad T, Blanquart C, Gonzalez-Yanes C (2007) The use of bioluminescence resonance energy transfer for the study of therapeutic targets: application to tyrosine kinase receptors. *Expert Opin Ther Targets* 11: 541–556.
27. Siddiqui S, Cong WN, Daimon CM, Martin B, Maudsley S (2013) BRET Biosensor Analysis of Receptor Tyrosine Kinase Functionality. *Front Endocrinol (Lausanne)* 4: 46.
28. De Meyts P (2008) The insulin receptor: a prototype for dimeric, allosteric membrane receptors? *Trends Biochem Sci* 33: 376–384.
29. Boute N, Pernet K, Issad T (2001) Monitoring the activation state of the insulin receptor using bioluminescence resonance energy transfer. *Mol Pharmacol* 60: 640–645.
30. Issad T, Boute N, Pernet K (2002) The activity of the insulin receptor assessed by bioluminescence resonance energy transfer. *Ann N Y Acad Sci* 973: 120–123.
31. Issad T, Boute N, Pernet K (2002) A homogenous assay to monitor the activity of the insulin receptor using Bioluminescence Resonance Energy Transfer. *Biochem Pharmacol* 64: 813–817.
32. Boute N, Boubekeur S, Lacasa D, Issad T (2003) Dynamics of the interaction between the insulin receptor and protein tyrosine-phosphatase 1B in living cells. *EMBO Rep* 4: 313–319.
33. Nouaille S, Blanquart C, Zilberfarb V, Boute N, Perdureau D, et al. (2006) Interaction between the insulin receptor and Grb14: a dynamic study in living cells using BRET. *Biochem Pharmacol* 72: 1355–1366.
34. Kulahin N, Sanni SJ, Slaaby R, Nohr J, Gammeltoft S, et al. (2012) A BRET assay for monitoring insulin receptor interactions and ligand pharmacology. *J Recept Signal Transduct Res* 32: 57–64.
35. Kim JG, Kang MJ, Yoon YK, Kim HP, Park J, et al. (2012) Heterodimerization of glycosylated insulin-like growth factor-1 receptors and insulin receptors in cancer cells sensitive to anti-IGF1R antibody. *PLoS One* 7: e33322.
36. Flajolet M, Wang Z, Futter M, Shen W, Nuangchamnon N, et al. (2008) FGF acts as a co-transmitter through adenosine A2A receptor to regulate synaptic plasticity. *Nat Neurosci* 11: 1402–1409.
37. Maudsley S, Pierce KL, Zamah AM, Miller WE, Ahn S, et al. (2000) The β -adrenergic receptor mediates extracellular signal-regulated kinase activation via assembly of a multi-receptor complex with the epidermal growth factor receptor. *J Biol Chem* 275: 9572–9580.
38. Waters CM, Connell MC, Pyne S, Pyne NJ (2005) c-Src is involved in regulating signal transmission from PDGF β receptor-GPCR(s) complexes in mammalian cells. *Cell Signal* 17: 263–277.
39. Wang C, Buck DC, Yang R, Macey TA, Neve KA (2005) Dopamine D2 receptor stimulation of mitogen-activated protein kinases mediated by cell type-dependent transactivation of receptor tyrosine kinases. *J Neurochem* 93: 899–909.
40. Borroto-Escuela DO, Tarakanov AO, Guidolin D, Ciruela F, Agnati LF, et al. (2011) Moonlighting characteristics of G protein-coupled receptors: focus on receptor heteromers and relevance for neurodegeneration. *IUBMB Life* 63: 463–472.
41. Veljkovic V, Cosic I (1987) A novel method of protein analysis for prediction of biological function: application to tumor toxins. *Cancer Biochem Biophys* 9: 139–148.
42. Veljkovic V, Cosic I, Dimitrijevic B, Lalovic D (1985) Is it possible to analyze DNA and protein sequences by the methods of digital signal processing? *IEEE Trans Biomed Eng* 32: 337–341.
43. Doliana R, Veljkovic V, Prljic J, Veljkovic N, De Lorenzo E, et al. (2008) EMILINs interact with anthrax protective antigen and inhibit toxin action in vitro. *Matrix Biol* 27: 96–106.
44. Mancini M, Veljkovic N, Leo E, Aluigi M, Borsi E, et al. (2012) Cytoplasmic compartmentalization by Bcr-Abl promotes TET2 loss-of-function in chronic myeloid leukemia. *J Cell Biochem* 113: 2765–2774.
45. Svendsen AM, Vrecl M, Ellis TM, Heding A, Kristensen JB, et al. (2008) Cooperative binding of insulin-like Peptide 3 to a dimeric relaxin family peptide receptor 2. *Endocrinology* 149: 1113–1120.
46. Vrecl M, Norregaard PK, Almholst DL, Elster L, Pogacnik A, et al. (2009) β -arrestin-based BRET² screening assay for the “non”- β -arrestin binding CB1 receptor. *J Biomol Screen* 14: 371–380.
47. Vrecl M, Jorgensen R, Pogacnik A, Heding A (2004) Development of a BRET² screening assay using β -arrestin 2 mutants. *J Biomol Screen* 9: 322–333.
48. Ramsay D, Kellett E, McVey M, Rees S, Milligan G (2002) Homo- and hetero-oligomeric interactions between G-protein-coupled receptors in living cells monitored by two variants of bioluminescence resonance energy transfer (BRET): hetero-oligomers between receptor subtypes form more efficiently than between less closely related sequences. *Biochem J* 365: 429–440.
49. Kubale V, Abramovic Z, Pogacnik A, Heding A, Sentjurc M, et al. (2007) Evidence for a role of caveolin-1 in neurokinin-1 receptor plasma-membrane localization, efficient signaling, and interaction with β -arrestin 2. *Cell Tissue Res* 330: 231–245.
50. Veatch W, Stryer L (1977) The dimeric nature of the gramicidin A transmembrane channel: conductance and fluorescence energy transfer studies of hybrid channels. *Journal of molecular biology* 113: 89–102.
51. Veljkovic N, Glisic S, Prljic J, Perovic V, Botta M, et al. (2008) Discovery of new therapeutic targets by the informational spectrum method. *Curr Protein Pept Sci* 9: 493–506.
52. Veljkovic V, Niman HL, Glisic S, Veljkovic N, Perovic V, et al. (2009) Identification of hemagglutinin structural domain and polymorphisms which may modulate swine H1N1 interactions with human receptor. *BMC Struct Biol* 9: 62.
53. Veljkovic V, Veljkovic N, Muller CP, Muller S, Glisic S, et al. (2009) Characterization of conserved properties of hemagglutinin of H5N1 and human influenza viruses: possible consequences for therapy and infection control. *BMC Struct Biol* 9: 21.
54. Drinovec L, Kubale V, Nohr Larsen J, Vrecl M (2012) Mathematical models for quantitative assessment of bioluminescence resonance energy transfer: application to seven transmembrane receptors oligomerization. *Front Endocrinol (Lausanne)* 3: 104.
55. Calebiro D, Rieken F, Wagner J, Sungkaworn T, Zabel U, et al. (2013) Single-molecule analysis of fluorescently labeled G-protein-coupled receptors reveals complexes with distinct dynamics and organization. *Proc Natl Acad Sci U S A* 110: 743–748.
56. Ferre S, Casado V, Devi LA, Filizola M, Jockers R, et al. (2014) G Protein-Coupled Receptor Oligomerization Revisited: Functional and Pharmacological Perspectives. *Pharmacol Rev* 66: 413–434.
57. Scarselli M, Donaldson JG (2009) Constitutive internalization of G protein-coupled receptors and G proteins via clathrin-independent endocytosis. *J Biol Chem* 284: 3577–3585.
58. Oakley RH, Laporte SA, Holt JA, Barak LS, Caron MG (1999) Association of β -arrestin with G protein-coupled receptors during clathrin-mediated endocytosis dictates the profile of receptor resensitization. *J Biol Chem* 274: 32248–32257.
59. Seachrist JL, Anborgh PH, Ferguson SS (2000) β_2 -adrenergic receptor internalization, endosomal sorting, and plasma membrane recycling are regulated by rab GTPases. *J Biol Chem* 275: 27221–27228.
60. Di Certo MG, Batassa EM, Casella I, Serafino A, Floridi A, et al. (2008) Delayed internalization and lack of recycling in a β_2 -adrenergic receptor fused to the G protein alpha-subunit. *BMC Cell Biol* 9: 56.
61. Karoor V, Wang L, Wang HY, Malbon CC (1998) Insulin stimulates sequestration of β -adrenergic receptors and enhanced association of β -adrenergic receptors with Grb2 via tyrosine 350. *J Biol Chem* 273: 33035–33041.
62. Gavi S, Yin D, Shumay E, Wang HY, Malbon CC (2005) The 15-amino acid motif of the C terminus of the β_2 -adrenergic receptor is sufficient to confer

- insulin-stimulated counterregulation to the β_1 -adrenergic receptor. *Endocrinology* 146: 450–457.
63. Dacres H, Michie M, Wang J, Pflieger KD, Trowell SC (2012) Effect of enhanced Renilla luciferase and fluorescent protein variants on the Forster distance of Bioluminescence resonance energy transfer (BRET). *Biochem Biophys Res Commun* 425: 625–629.
 64. Mondal S, Johnston JM, Wang H, Khelashvili G, Filizola M, et al. (2013) Membrane driven spatial organization of GPCRs. *Sci Rep* 3: 2909.
 65. Ayoub MA, Levoe A, Delagrang P, Jockers R (2004) Preferential formation of MT₁/MT₂ melatonin receptor heterodimers with distinct ligand interaction properties compared with MT₂ homodimers. *Mol Pharmacol* 66: 312–321.
 66. Terrillon S, Durroux T, Mouillac B, Breit A, Ayoub MA, et al. (2003) Oxytocin and vasopressin V1a and V2 receptors form constitutive homo- and heterodimers during biosynthesis. *Mol Endocrinol* 17: 677–691.
 67. Goin JC, Nathanson NM (2006) Quantitative analysis of muscarinic acetylcholine receptor homo- and heterodimerization in live cells: regulation of receptor down-regulation by heterodimerization. *J Biol Chem* 281: 5416–5425.
 68. Breitwieser GE (2004) G protein-coupled receptor oligomerization: implications for G protein activation and cell signaling. *Circ Res* 94: 17–27.
 69. Katragadda M, Maciejewski MW, Yeagle PL (2004) Structural studies of the putative helix 8 in the human β_2 adrenergic receptor: an NMR study. *Biochim Biophys Acta* 1663: 74–81.
 70. Ghosh A, Sonavane U, Joshi R (2014) Multiscale modelling to understand the self-assembly mechanism of human β_2 -adrenergic receptor in lipid bilayer. *Comput Biol Chem* 48: 29–39.
 71. Doronin S, Wang Hy HY, Malbon CC (2002) Insulin stimulates phosphorylation of the β_2 -adrenergic receptor by the insulin receptor, creating a potent feedback inhibitor of its tyrosine kinase. *J Biol Chem* 277: 10698–10703.
 72. Doronin S, Shumay E, Wang HY, Malbon CC (2002) Akt mediates sequestration of the β_2 -adrenergic receptor in response to insulin. *J Biol Chem* 277: 15124–15131.
 73. Mothe I, Tartare S, Kowalski-Chauvel A, Kaliman P, Van Obberghen E, et al. (1995) Tyrosine kinase activity of a chimeric insulin-like-growth-factor-1 receptor containing the insulin receptor C-terminal domain. Comparison with the tyrosine kinase activities of the insulin and insulin-like-growth-factor-1 receptors using a cell-free system. *Eur J Biochem* 228: 842–848.
 74. Soni P, Lakkis M, Poy MN, Fernstrom MA, Najjar SM (2000) The differential effects of pp120 (Ceacam 1) on the mitogenic action of insulin and insulin-like growth factor 1 are regulated by the nonconserved tyrosine 1316 in the insulin receptor. *Mol Cell Biol* 20: 3896–3905.
 75. Hubbard SR, Wei L, Ellis L, Hendrickson WA (1994) Crystal structure of the tyrosine kinase domain of the human insulin receptor. *Nature* 372: 746–754.
 76. Navarro G, Ferre S, Cordomi A, Moreno E, Mallol J, et al. (2010) Interactions between intracellular domains as key determinants of the quaternary structure and function of receptor heteromers. *J Biol Chem* 285: 27346–27359.